Flexible and Printed Electronics

PAPER

Profile improvement of blade coated circuits by the capillary force originating from the hydrophobic sidewalls

To cite this article: Cheng Tang *et al* 2024 *Flex. Print. Electron.* **9** 035009

Flexible and Printed Electronics

PAPER

Profile improvement of blade coated circuits by the capillary force originating from the hydrophobic sidewalls

Cheng Tang[1,2], Rui Liu[1,*], Shanyou Zhu[1,2], Subin Jiang[3,*], Ke Shui[2], Jian Lin[2,3,*] and Chang-Qi Ma[2,3,*]

[1] National Demonstration Center for Experimental Materials Science and Engineering Education, Jiangsu University of Science and Technology, Zhenjiang 212003, People's Republic of China
[2] Printable Electronics Research Centre, Suzhou Institute of Nano-tech and Nano-bionics, Chinese Academy of Sciences, Suzhou Industrial Park, Suzhou, Jiangsu Province 215123, People's Republic of China
[3] Engineering Center of Precision Printing Manufacturing, Guangdong Institute of Semiconductor Micro-Nano Manufacturing Technology, Kejiao Road No. 1, Shishan Town, Foshan 528225 , People's Republic of China
* Authors to whom any correspondence should be addressed.

E-mail: liurui@just.edu.cn, sbjiang2022@sinanogd.ac.cn, jlin2010@sinano.ac.cn and cqma2011@sinano.ac.cn

Keywords: hydrophobic sidewalls, profile improvement, coffee ring, micro-channel

Supplementary material for this article is available online

RECEIVED
14 February 2024

REVISED
18 August 2024

ACCEPTED FOR PUBLICATION
9 September 2024

PUBLISHED
26 September 2024

Abstract

Restricting the diffusion of conductive inks plays a key role in printed electronics application. Micro-channels with different sidewall surface energies, which can be approximated as a capillary, are fabricated to restrict the blade-coated ink diffusion using both of the gravitational effect and the capillary force. The coffee ring effect of aqueous silver ink is inhibited by the capillary force when the hydrophobic sidewalls distance is no more than 50 μm in this paper. As a result, the conductive lines with improved cross-sectional profiles are obtained by this method, with the typical resistivity more than 10^8 times lower than the measured results with hydrophilic sidewalls. The capillary force was also found to lose its effect when the width is larger enough, which needs surfactant addition to improve the silver film property. *I–V* curves of the original aqueous ink and the ink improved by traditional methods shows that the profile improvement by the hydrophobic sidewall can be used with other ink improving methods cooperatively. These studies open up the possibility of improving the printed conductive patterns by this method as an auxiliary tool used together with the traditional methods reported before.

1. Introduction

Printed electronics represent a novel technology that is applicable to produce electronic devices through conventional printing processes [1, 2]. It shows various advantages such as low cost, simple process and environmental friendliness. Different functional nanomaterials are made into ink, which are deposited on the substrates as electronic functional films with a specific pattern [3]. The fabrication of various new sensors by printing method is widely reported in the production of electronics to simplify the process, reduce energy consumption and increase productivity [4, 5]. Currently, the main forces in electronics-printing technologies include screen printing, inkjet printing, doctor blade coating and so on [6, 7].

Despite the aforementioned advantages of printed electronics, it has not yet been widely applied in mass production [8, 9]. Two of the biggest obstacles limiting its application are the concave profiles in the cross-section mostly due to the coffee ring effect, as well as the fine patterns no more than 50 μm [10, 11] because of the ink flow and spreading on substrate. As a result, how to improve the cross-sectional profiles and resolutions are two important research direction of modern electronic additive manufacturing [12]. It is necessary to search useful methods as much as possible for the widely application of printed electronics in the future.

To suppress the concave cross-sectional profiles with the coffee ring effect, various methods have been reported including controlling the substrate temperatures [13], shape-dependent capillary interactions [14], photoresponsive suspension composed of anionic colloids and a photosensitive surfactant [15], and sugar-assisted depinning of contact line [16].

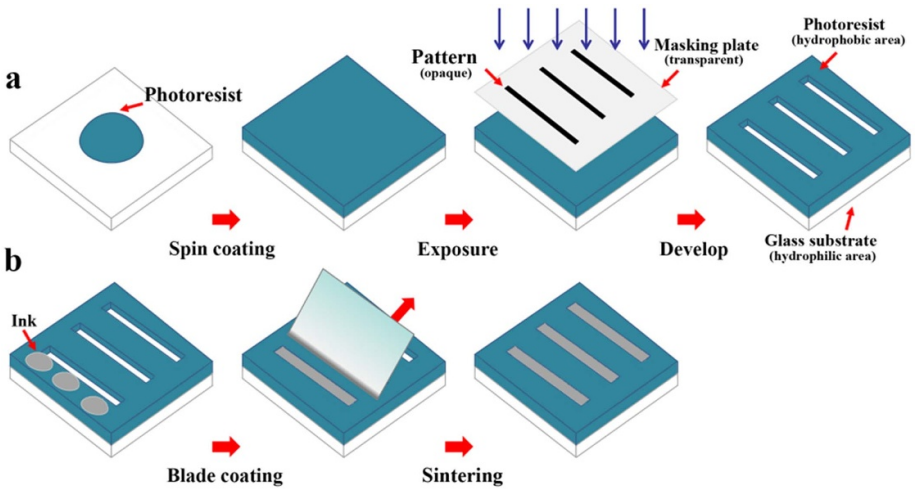

Figure 1. Steps of pattern fabrication and printing. (a) Schematic diagram of the micro-channels fabrication process with different surface energies, and (b) schematic diagram of ink blade coating.

On the other hand, the resolution improvement of the additive printed circuits has been reported by restricting ink flow using the difference of surface energy [17, 18] or height [19, 20]. It is crucial to improve printing resolution by constructing hydrophilic and hydrophobic boundaries to limit the diffusion of ink at the edges of the pattern [21]. When a droplet is at the junction of hydrophilic and hydrophobic surface, it will move from the hydrophobic regions to the hydrophilic area [22].

The conductive ink can also be scraped or printed into the micro-channels fabricated by hot-embossing [19] or ultraviolet-nanoimprint lithography [20, 23]. Most substrates and sidewalls of reported micro-channels for conductive ink filling have similar surface energies. The plasma treatment was even used to make sure the substrates and sidewalls are hydrophilic enough [20]. On the other hand, it is possible to improve the ink diffusion restriction utilizing the capillary force if the channel sidewall is much more hydrophobic than the substrate surface according to the reports using hydrophilic–hydrophobic boundaries to control the ink flow [18]. However, there has been seldom report to study the impact of channels with different surface energies on ink flow yet. More importantly, such kinds of method can be used in together with the traditional ink improved methods reported before.

In this paper, it is proposed to construct hydrophobic sidewalls by a hydrophobic photoresist layer on a hydrophilic glass substrate, which means the fabricated micro-channels can restrict the blade-coated ink diffusion using both of the gravitational effect and the capillary force. The aqueous nanosilver conductive ink in the micro-channels was then dried to form a conductive thin film. Coffee ring effect of blade-coated aqueous silver ink is found to be suppressed due to the capillary force when the distance of hydrophobic sidewalls is no more than 50 μm.

2. Experimental section

2.1. Material preparation

The nanosilver conductive ink (35–40 wt%) comes from BroadTeko, with the silver particle size of 30–50 nm diameter. The specific parameters are shown in table S1. KYC-511 comes from Keying Chemical and the solvent is ethylene glycol. Polyethylene glycol (PEG) and diethylene glycol methyl are purchased from Aladdin reagent. The photoresist for micro-channels fabrication is purchased from Dai Nippon Printing Co., Ltd All chemicals were used without further purification.

2.2. Experimental procedure

Figure 1(a) shows the process of micro-channel fabrication. Firstly, the photoresist is used to develop a uniform film on the glass substrate through spin coating (shown in table S2). Then, the films were heated and baked on a hot plate at 85 °C for 2 min to remove the solvents from the photoresist and to enhance the adhesion between the photoresist and substrate [24]. The desired pattern is obtained by means of mask-aligned exposure, and the photoresist is cured by 365 nm UV irradiation after 5 s of exposure. Then the parts that have not been exposed to UV light are removed after development, with the glass substrate uncovered as the hydrophilic area. While a hydrophobic region develops in the region cured by UV light irradiation, with the masked pattern and photoresist pattern at a ratio of 1:1. The patterns produced through photolithography using an exposure time for 5 s and a development time for 60 s. Next, the silver ink is filled into the pattern

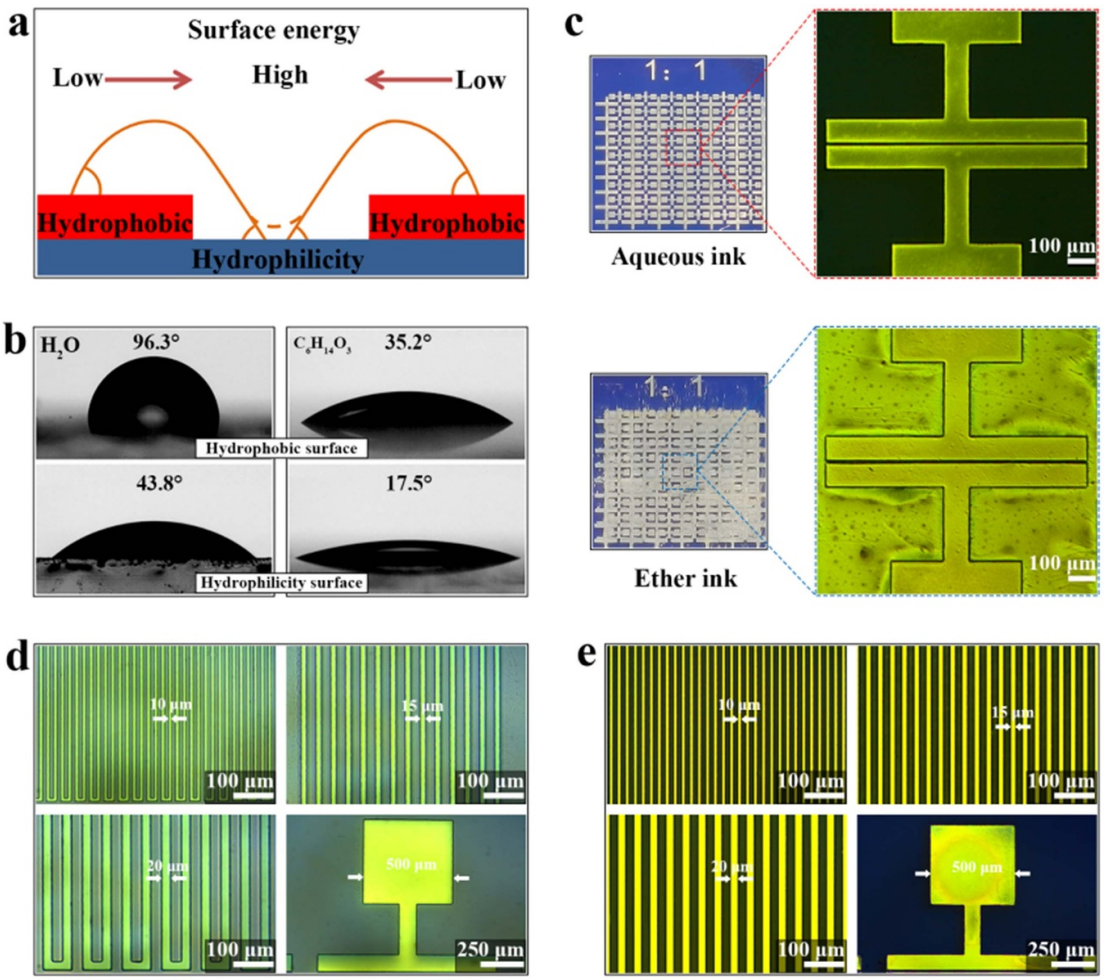

Figure 2. (a) Basic mechanism of ink movement on the surface with different surface energies. (b) Contact angles of water and diethylene glycol methyl ether on the different surfaces. (c) Comparison of blade-coating effects of aqueous and ether inks. (d) Optical micrographs of micro-channel patterns with different widths of 10, 15, 20, and 500 μm, respectively. (e) Optical microscopic images of samples with the blade-coated silver conductive ink.

formed by the photoresist through scraping, as shown in figure 1(b). The coating machine is ZAA2300 produced by Zehntner company, and its scraping speed is 1–99 mm s^{-1}. In order to fully fill the ink into the pattern, the optimal scraping speed was determined through multiple experiments to be 1 mm s^{-1}, and the optimal distance between the scraper and the pattern was 20 μms. After ink self-assembly, the formed electronic circuits are directly dried under environmental conditions for 30 min, and then sintered at 250 °C for 2 h.

The morphology of ink film formation was observed and analyzed using optical microscopy and atomic force microscope (AFM, Asylum Research MFP-3D). The accumulation of silver particles after ink film dried was observed using scanning electron microscope (Regulus SU8230). We use contact angle testers (SinDin Precision SDC-200 S), surface tension testers (Kibron EZ-Piplus), thermogravimetric analyzers (Mettler DSC3), and rheometers (Kinexus Lab+) to analyze the parameters of ink with different additives. The *I*–*V* curves were obtained using a probe stage with a Keithley 2636 sourcemeter.

3. Results and discussion

3.1. Application of micro-channels with hydrophilic and hydrophobic sidewalls

By means of blade-coating, the ink is filled into the micro-channels and then dried as a thin solid silver layer, with almost no silver remained in the photoresist area. The result from the tendency of droplets to spread out at the interfaces with high surface energy, i.e., the occurrence of 'wetting'. At the interfaces with low surface energy, however, they tend to shrink, i.e., the occurrence of 'dewetting' movement. The surface energy differences used to assist printing are based on the sudden change in surface energy between the neighboring regions at a solid interface, which provides a well-defined driving force on the ink droplets [25]. As shown in figure 2(a), at the interface of surface energy difference, the contact angle of a droplet is smaller when it is at the interface of a solid

with a high surface energy, but larger when it is at the interface of a solid with a low surface energy [26]. When the droplet is located at this difference demarcation line, it shifts towards the higher surface energy of the solid–liquid interface due to the direct pulling effect caused by the solid–liquid interfacial tension. Thus, the droplet shifts from the hydrophobic region to the hydrophilic region.

Water and diethylene glycol methyl ether are commonly used solvents for silver conductive inks. The contact angles of them in the hydrophilic and hydrophobic regions were tested separately below, as shown in figure 2(b). The difference of contact angles is insignificant for the diethylene glycol methyl ether on the hydrophilic and hydrophobic patterns, while the difference of water contact angles is sufficient. As shown in figure 2(c), there is no residual of water-based ink in the hydrophobic regions while it can be filled into the hydrophilic patterns. However, the ether-based ink hinders the distinction between the hydrophilic and hydrophobic regions, which cannot be used to distinguish the regions with different surface energy. Finally, the aqueous nanosilver conductive ink is used for the study, and the pattern obtained before blade coating is shown in figure 2(d). The finally obtained pattern is shown in figure 2(e), with the minimum line width of 10 μm.

3.2. The different silver cross-sectional profiles in micro-channels with hydrophilic and hydrophobic sidewalls

In order to distinguish the role of the hydrophobic sidewall in the morphology formation of the dried ink, the hydrophobic sidewall of micro-channels were turned into hydrophilic using the plasma treatment, as shown in figure 3(a). However, the area of sidewall is too small for the contact angle measurement. Considering the surface energy of the photoresist material is mainly determined by the surface topography and surface chemistry [27], the measured contact angle of the sidewall surface has the same value as the top area of the photoresist sample because of the same material. As a result, the measured contact angles on the photoresist top area were used to instead the contact angles on the sidewall surface. The comparison of the measured water contact angles before and after the plasma treatment can be seen in figure 3(b).

On the other hand, figure 3(c) shows the morphology of blade-coated silver film in micro-channels with the widths of 10, 20, 30, 40, and 50 μm, which were observed. It can be found that the morphology of dried silver layer is concave because of the coffee ring effect during the solvent evaporation when the surface of sidewall is hydrophilic. In contrast, there is no coffee ring effect if the sidewalls have hydrophobic surfaces, which means a quite interesting result for

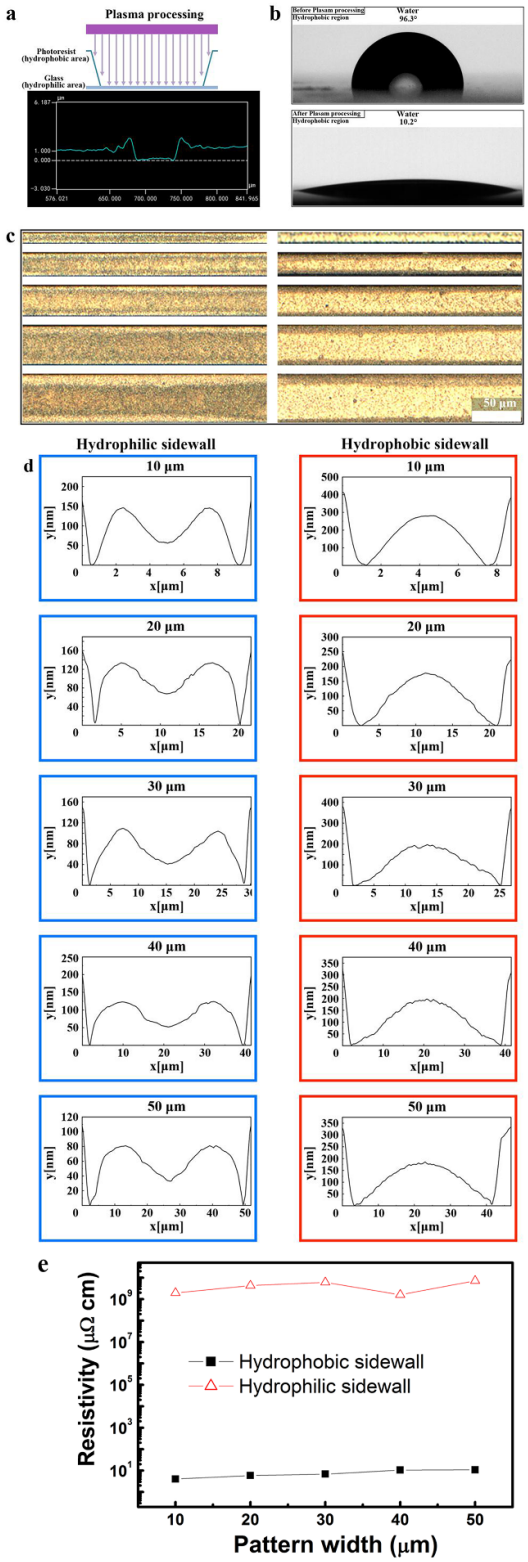

Figure 3. (a) Transformation of hydrophobic sidewalls into hydrophilic using Plasma treatment; (b) comparison of the water contact angles in hydrophobic regions before and after plasma treatment; (c) comparisons of blade-coated silver morphologies with hydrophilic and hydrophobic sidewalls with the channel widths of 10, 20, 30, 40, and 50 μm; (d) comparisons of AFM images of ink film-forming cross-sectional profile with hydrophobic and hydrophobic sidewalls; (e) comparison of the typical resistivity of the samples with hydrophilic and hydrophobic sidewalls.

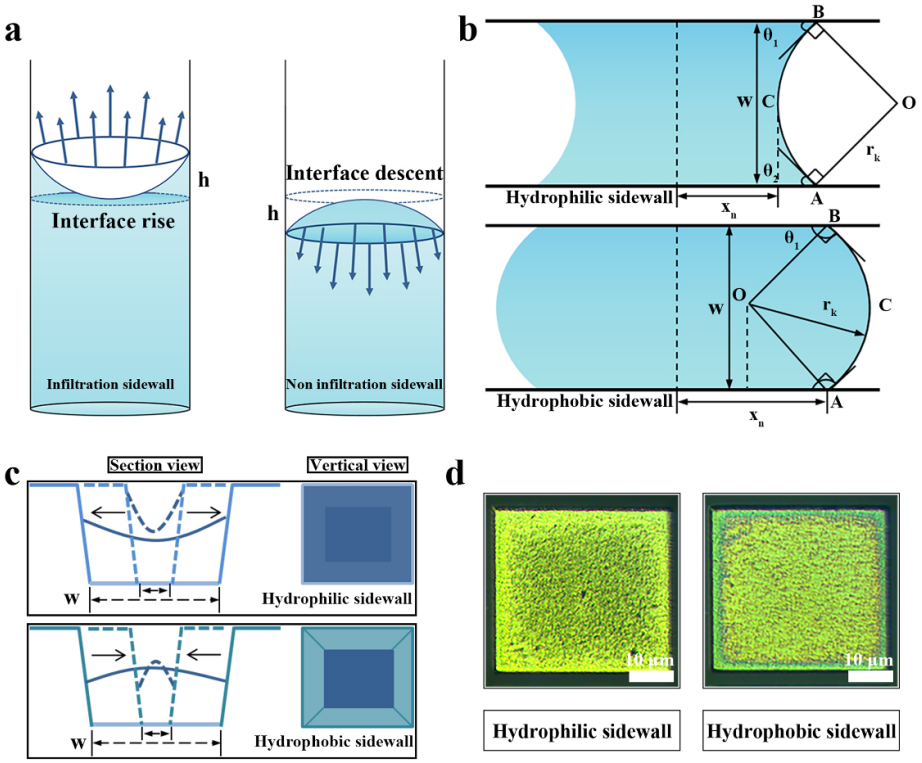

Figure 4. Schematic diagrams (a) and force analysis (b) of the liquid with the hydrophilic and hydrophobic sidewalls. (c) Influence of the capillary during the film formation of the ink. (d) Comparison of the film formation of the hydrophilic and hydrophobic sidewalls under optical microscope.

the cross-sectional profile improvement of the silver deposition. Compared to the images of film morphology with hydrophobic sidewall, it can be found out that the accumulation of ink expands towards the edges of the pattern when the sidewall is hydrophilic, with the silver particles in central region reduced obviously.

Figure 3(d) shows the AFM measured cross-sectional profiles of the blade-coated silver ink with hydrophilic and hydrophobic sidewalls at 10 μm, 20 μm, 30 μm, 40 μm, and 50 μm, respectively. It is found out that the film formed by the ink with hydrophilic sidewalls shows a profile with more silver particles on both sides and less in the middle, which leads to an obvious coffee ring morphology. On the other hand, there were obviously convex cross-sectional profiles without coffee ring effects for the dried ink with hydrophobic sidewalls. Considering the printed thin lines with convex cross-sectional profiles have more stable electrical conductivity than those with concave contours [28], this kind of silver patterns is much better for the printed electronics applications. Figure 3(e) also confirms that conductive lines obtained using hydrophobic sidewalls have typical resistivity more than 10^8 times lower than the measured results with hydrophilic sidewalls.

3.3. The capillary forces and meniscus of filled ink with sidewalls

To explain the different cross-sectional profiles of silver in figure 3, the different capillary forces with hydrophilic or hydrophobic sidewalls are studied assuming that the micro-channel sidewalls play the roles as traditional capillary tube walls (shown in figure 4(a)). As a result, the liquid is subjected to capillary forces as the capillary channels are filled. At the solid–liquid interface, these two forces are applied at the same time with different magnitudes [29]. If the capillary sidewall is made of hydrophilic material, a concave meniscus was formed because the adhesion force between capillary sidewall and liquid molecules is greater than the cohesion force between the liquid molecules. On the contrary, there is a convex meniscus [30, 31] if the capillary sidewall to the liquid is made of hydrophobic material. According to the Young–Laplace formula, the magnitude of the pressure of the meniscus liquid surface pressure subjected to capillary action is expressed as

$$P = \frac{2\gamma\cos\theta}{R}. \quad (1)$$

(Among γ is the surface tension of the liquid, θ is the cosine of the angle between the liquid and the pipe wall, where R is the radius of the pipe).

As a result, it can be inferred that the hydrophobic sidewall with a certain height can keep the convex meniscus during the film-forming process, which inhibits the coffee ring effect by balancing the flows and finally improves the cross-sectional profile of the dried film. On the other hand, P and R are inversely proportional, which means that a larger width will make the meniscus between sidewalls more flat.

According to the model proposed by Liu *et al* [31] about different meniscus shapes obtained as a result of different hydrophilic/hydrophobic properties and separate distances, the width of micro-channel (shown in figure 4(b)) can be expressed as

$$w = r_k\left(\cos\theta_1 + \cos\theta_2\right). \tag{2}$$

(Among r_k is the radius of the meniscus, θ_1 and θ_2 are the contact angles between the liquid and the sidewalls).

It can be found that the radius of the meniscus will increased with the micro-channel width, which also means the meniscus between sidewalls becoming more flat.

Influence of the capillary during the film formation can also be verified by the comparison in figures 4(c) and (d). The dried silver ink surrounded with the hydrophilic sidewalls has obvious coffee ring effect, while the hydrophobic sidewalls can suppresses the coffee ring effect during the ink dry process.

3.4. The coffee ring inhibition for larger patterns

As mentioned above, the convex meniscus between hydrophobic sidewalls will become more flat when the width of micro-channel increasing. It also means that the meniscus between sidewalls does not play their special role in coffee ring inhibition. Then the silver profiles in the cross-section became concave due to the coffee ring effect [32], as shown in the left of figure 5(a). This effect is a complex process influenced by various factors such as the surface tension, viscosity, and solid content of the ink itself [14, 33, 34].

To confirm if our proposed method by the hydrophobic sidewall can be used as an auxiliary tool together with other methods, the conductive silver ink improved using traditional methods to avoid coffee ring effect is also necessary. The surfactant, which has low surface tension and high boiling point, is usually added into the ink to inhibit the coffee ring effect [35]. It plays the key role in dried film morphology improvement when the Marangoni flow and the capillary flow are balanced, as shown in the right of figure 5(a).

To suppress the coffee ring effect, PEG and leveling agent KYC-511 (the solvent is ethylene glycol, and the main component is non-silicon surfactant) are taken as additives. The contact angle difference between hydrophilic and hydrophobic patterns for these two reagents is large enough (figure S3). Adding a small amount of leveling agent will increase the viscosity of the ink and significantly reduce the surface tension of the ink, which can inhibit the coffee ring effect obviously. But the increase in viscosity and the decrease in surface tension may also make the ink moving from hydrophobic to hydrophilic regions more hard.

Although PEG can also reduce the surface tension of ink, it requires a large amount of addition, which can increase the viscosity of ink and make it difficult to distinguish hydrophilic and hydrophobic patterns (figure S4). In order to ensure the accuracy of the printed pattern, two optimized ink samples with 5 wt% PEG or 0.5 wt% leveling agent were ultimately selected for preparation.

The shear viscosities of the samples were measured and compared as a function of shear rates in figure 5(b). On the other hand, figure 5(c) shows that the addition of PEG does not affect the surface tension of the inks, while the addition of KYC-511 reduces the ink surface tension sharply.

It can be found from figures 5(d) and (e) that the films formed by different ink samples have distinct morphologies and conductivities because of the additives. The water-based inks without any additive has very uniformly dried morphology because of the 500 μm hydrophobic sidewalls distance. The measured resistance of this sample is also as high as 7.69×10^9 Ω, with the calculated resistivity of 9.2×10^8 $\mu\Omega$ cm.

The dried film sample with 5 wt% of PEG has a higher measured resistance of 8.55×10^9 Ω though there is reduced coffee ring effect because of the additive, with the calculated resistivity of 1.0×10^9 $\mu\Omega$ cm. We believe that the decreased shear viscosity and similar surface tension making the ink cannot spread very well, which leads to the flow defects including fish-eye and shrinkage. And PEG exists in the film, making it difficult to completely remove it by heating (figure S5). On the other hand, the sample with the addition of 0.5 wt% KYC-511, which has a very smooth film morphology, has a sudden decreased resistance of 27.8 Ω, with the calculated resistivity of 3.3 $\mu\Omega$ cm. Besides the inhibited coffee ring effect, increased shear viscosity and similar surface tension of the ink should also plays their key roles.

In order to verify the effect of the printed silver lines improvement caused by our method, the resistance is measured using the two-point probe method (figure 6(a)) after ink film formation in

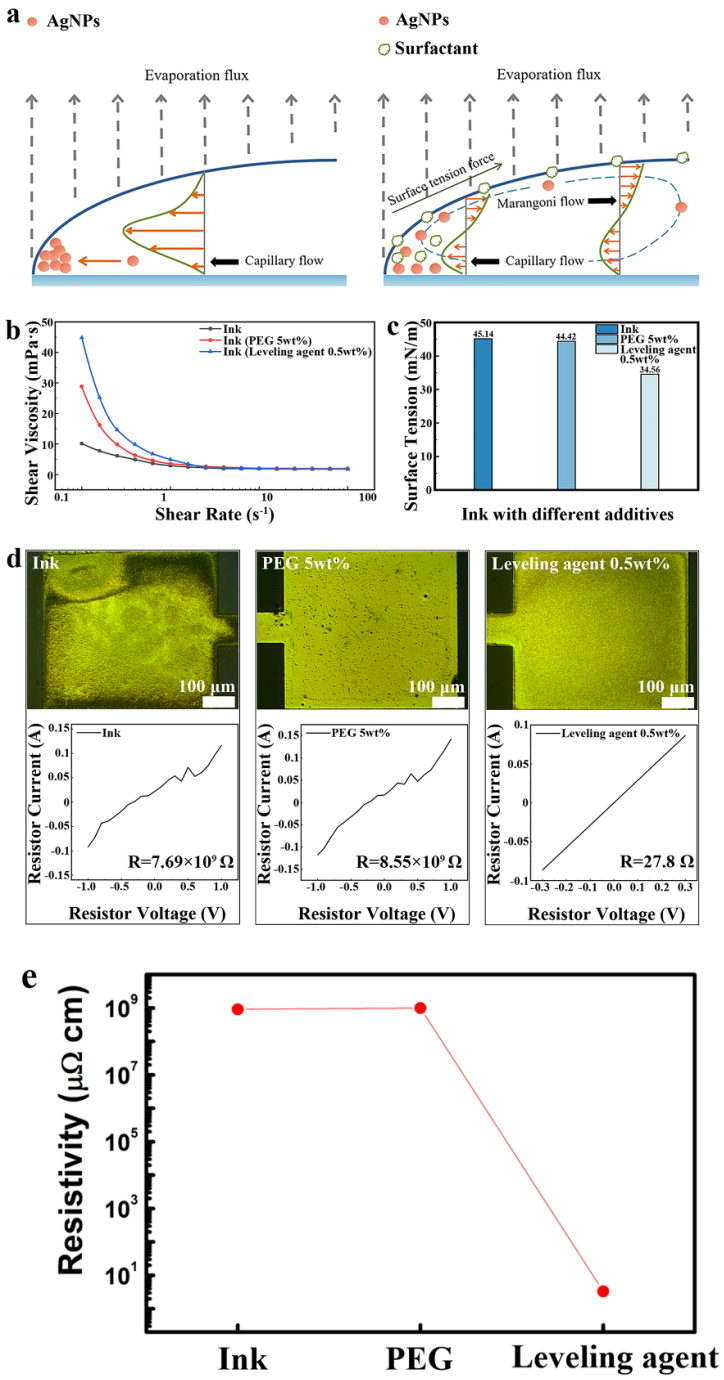

Figure 5. (a) Left: schematic of the coffee ring effect right: inhibition of the coffee ring effect by addition of surfactants. The comparison of viscosity (b) and surface tension (c) changes of aqueous conductive inks. (d) Optical microscope morphology of the three inks after film formation in a 500 μm hydrophobic sidewalls and the *I–V* curves measured by the probe stage. (e) The calculated resistivity of the different samples.

the micro-channels of different widths (10–50 μm) given the constant length (450 μm) [36]. Also, the effect of pattern width on the ink film formation is analyzed by comparing the differences in the electrical properties of the formed films. Figures 6(b)–(d) show the *I–V* curves of aqueous ink, the ink added with PEG, and the ink added with leveling agent at different widths, respectively. These results also confirm that the profile improvement by the hydrophobic sidewall can be used as an auxiliary tool together with the traditional ink improving methods.

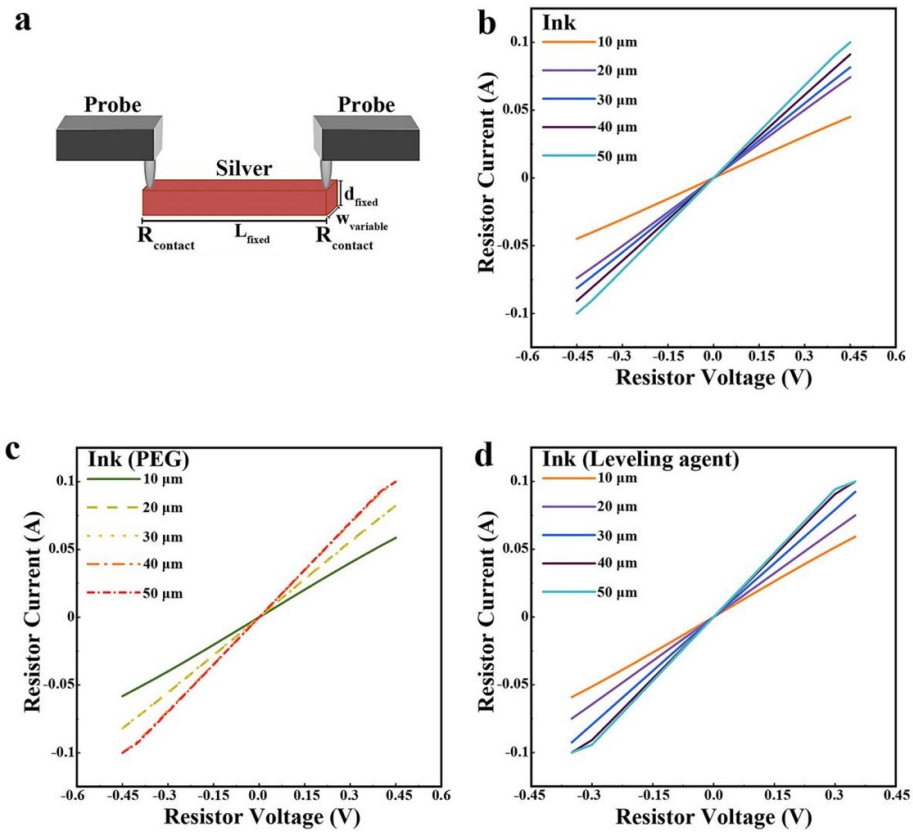

Figure 6. (a) Schematic diagram of the two-point probe method for measuring wire resistance. The *I–V* curves of aqueous silver conductive ink (b), ink with the addition of PEG (c), and ink with the addition of leveling agent (d).

4. Conclusions

In summary, micro-channels with different sidewall surface energies are fabricated for restricting the ink diffusion by both of the gravitational effect and the capillary force. Conductive patterns with improved cross-sectional profiles are obtained by blade-coated aqueous nanosilver ink into these channels. It can be found that the coffee ring effect of blade-coated aqueous silver ink is suppressed due to the capillary force if the hydrophobic sidewalls distance is no more than 50 μm. The capillary force also loses its effect if the distance of the hydrophobic sidewalls increased to be 500 μm. It is necessary to suppress the reappeared coffee ring effect and improve the silver film properties by adding surfactant into the ink. The measured resistance of samples with the same pattern was found to decrease from 7.69×10^9 Ω to 27.8 Ω. The reported method, that improving the profile of blade coated circuits by the capillary force originating from the hydrophobic sidewalls with no more than 50 μm, has provided a solution to both of the two biggest obstacles mentioned in the introduction part. More importantly, this method can be seen as an auxiliary tool used cooperatively with the traditional ink improved methods for improved cross-sectional profile and resolution. It opens up the possibility of high-resolution blade coated electronics widely applied in mass production.

Data availability statement

All data that support the findings of this study are included within the article (and any supplementary files).

Acknowledgments

This work was supported by Guangdong Basic and Applied Basic Research Foundation (Grant No. 2020B1515120059), Foshan post-doctoral foundation (No.2022BA09000).

ORCID iDs

Jian Lin https://orcid.org/0000-0002-3037-7023
Chang-Qi Ma https://orcid.org/0000-0002-9293-5027

References

[1] Khan S, Lorenzelli L and Dahiya R S 2015 Technologies for printing sensors and electronics over large flexible substrates: a review *IEEE Sens. J.* **15** 3164–85

[2] Khan Y, Thielens A, Muin S, Ting J, Baumbauer C and Arias A C 2020 A new frontier of printed electronics: flexible hybrid electronics *Adv. Mater.* **32** 1905279
[3] Chen S and Liu J 2022 Liquid metal printed electronics towards ubiquitous electrical engineering *Jpn. J. Appl. Phys.* **61** SE0801
[4] Zhuo Z, Bing L, Shaojie Z, Tongkun L and Jie C 2022 Battery screen print defect detection based on stationary velocity fields neural network matching and optical flow rectification *Rev. Sci. Instrum.* **93** 115110
[5] Moonen P F, Yakimets I and Huskens J 2012 Fabrication of transistors on flexible substrates: from mass-printing to high-resolution alternative lithography strategies *Adv. Mater.* **24** 5526–41
[6] Salaoru I, Maswoud S and Paul S 2019 Inkjet printing of functional electronic memory cells: a step forward to green electronics *Micromachines* **10** 417
[7] Zhou Y *et al* 2012 A universal method to produce low-work function electrodes for organic electronics *Science* **336** 327–32
[8] Sánchez A, Shalan A, Rosales M, Ruiz De Larramendi I and Campo F 2022 Screen-printed nickel hydroxide electrodes: semiconducting, electrocatalytic, and electrochromic properties *J. Electroanal. Chem.* **928** 117052
[9] Li L, Li W, Sun Q, Liu X, Jiu J, Tenjimbayashi M, Kanehara M, Nakayama T and Minari T 2021 Dual surface architectonics for directed self-assembly of ultrahigh-resolution electronics *Small* **17** e2101754
[10] Du X, Wankhede S P, Prasad S, Shehri A, Morse J and Lakal N 2022 A review of inkjet printing technology for personalized-healthcare wearable devices *J. Mater. Chem.* C **10** 14091–115
[11] Sun J, Sun R, Jia P, Ma M and Song Y 2022 Fabricating flexible conductive structures by printing techniques and printable conductive materials *J. Mater. Chem.* C **10** 9441–64
[12] Fukuda K and Someya T 2017 Recent progress in the development of printed thin-film transistors and circuits with high-resolution printing technology *Adv. Mater.* **29** 1602736
[13] Soltman D and Subramanian V 2008 Inkjet-printed line morphologies and temperature control of the coffee ring effect *Langmuir* **24** 2224–31
[14] Yunker P J, Still T, Lohr M A and Yodh A G 2011 Suppression of the coffee-ring effect by shape-dependent capillary interactions *Nature* **476** 308–11
[15] Manos A and Damien B 2014 Dynamic photocontrol of the coffee-ring effect with optically tunable particle stickiness *Angew. Chem., Int. Ed. Engl.* **53** 14077–81
[16] Shimobayashi S F, Tsudome M and Kurimura T 2018 Suppression of the coffee-ring effect by sugar-assisted depinning of contact line *Sci. Rep.* **8** 17769
[17] Schlisske S, Raths S, Ruiz-Preciado L A, Lemmer U, Exner K and Hernandez-Sosa G 2021 Surface energy patterning for ink-independent process optimization of inkjet-printed electronics *Flex. Print. Electron.* **6** 015002
[18] Shui K *et al* 2023 UV-converted heterogeneous wettability surface for the realization of printed micro-scale conductive circuits *Flex. Print. Electron.* **8** 035019
[19] Hendriks C E, Smith P J, Perelaer J, Van Den Berg A M J and Schubert U S 2008 “Invisible” silver tracks produced by combining hot-embossing and inkjet printing *Adv. Funct. Mater.* **18** 1031–8
[20] Wang Z, Yi P, Peng L, Lai X and Ni J 2017 Continuous fabrication of highly conductive and transparent Ag Mesh electrodes for flexible electronics *IEEE Trans. Nanotechnol.* **16** 687–94
[21] Jansen H P, Bliznyuk O, Kooij E S, Poelsema B and Zandvliet H J 2012 Simulating anisotropic droplet shapes on chemically striped patterned surfaces *Langmuir* **28** 499–505
[22] Vafaei S, Tuck C, Ashcroft I and Wildman R 2016 Surface microstructuring to modify wettability for 3D printing of nano-filled inks *Chem. Eng. Res. Des.* **109** 414–20
[23] J-l X, Liu Y-H, Gao X, Sun Y, Shen S, Cai X, Chen L and Wang S-D 2017 Embedded Ag grid electrodes as current collector for ultraflexible transparent solid-state supercapacitor *ACS Appl. Mater. Interfaces* **9** 27649–56
[24] Vijayamohanan H, Palermo E F and Ullal C K 2017 Spirothiopyran-based reversibly saturable photoresist *Chem. Mater.* **29** 4754–60
[25] Rossegger E, Hennen D, Griesser T, Roppolo I and Schlögl S 2019 Directed motion of water droplets on multi-gradient photopolymer surfaces *Polym. Chem.* **10** 1882–93
[26] Naderi P, Sheuten B R, Amirfazli A and Grau G 2023 Inkjet printing on hydrophobic surfaces: controlled pattern formation using sequential drying *J. Chem. Phys.* **159** 024712
[27] Walther F, Davydovskaya P, Zürcher S, Kaiser M, Herberg H, Gigler A M and Stark R W 2007 Stability of the hydrophilic behavior of oxygen plasma activated SU-8 *J. Micromech. Microeng.* **17** 524–31
[28] Fukuda K, Sekine T, Kumaki D and Tokito S 2013 Profile control of inkjet printed silver electrodes and their application to organic transistors *ACS Appl. Mater. Interfaces* **5** 3916–20
[29] Qin Z, Du Z, Xian Z and You H 2023 Theoretical and experimental study on capillary flow in a grooved microchannel with hydrophilic or hydrophobic walls *J. Fluids Struct.* **123** 103988
[30] Taesoo K and Kyubong J 2023 Microfluidic device to maximize capillary force driven flows for quantitative single-molecule DNA analysis *Biochip J.* **17** 384–92
[31] Liu -S-S, Zhang C-H and Liu J-M 2010 Calculation of meniscus force during separation of microsurfaces *Acta Phys. Sin.* **59** 6902–7
[32] Seo C, Jang D, Chae J and Shin S 2017 Altering the coffee-ring effect by adding a surfactant-like viscous polymer solution *Sci. Rep.* **7** 500
[33] Cui L, Zhang J, Zhang X, Huang L, Wang Z, Li Y, Gao H, Zhu S, Wang T and Yang B 2012 Suppression of the coffee ring effect by hydrosoluble polymer additives *ACS Appl. Mater. Interfaces* **4** 2775–80
[34] Xu T, Lam M L and Chen T-H 2017 Discrete element model for suppression of coffee-ring effect *Sci. Rep.* **7** 42817
[35] Anyfantakis M, Geng Z, Morel M, Rudiuk S and Baigl D 2015 Modulation of the coffee-ring effect in particle/surfactant mixtures: the importance of particle–interface interactions *Langmuir* **31** 4113–20
[36] Mahajan A, Hyun W J, Walker S B, Lewis J A, Francis L F and Frisbie C D 2015 High-resolution, high-aspect ratio conductive wires embedded in plastic substrates *ACS Appl. Mater. Interfaces* **7** 1841–7